MODELLING AND MANUFACTURING OF ACTUATABLE SHAPE MEMORY ALLOY HYBRID COMPOSITE PANELS

Sanesh Iyer, Pascal Hubert
McGill University
Department of Mechanical Engineering
Montreal, Quebec, H3A 0C3, Canada

ABSTRACT

Shape Memory Alloy Hybrid Composites (SMAHCs) are an exciting field of research for their potential to realize the dream of morphing structures. Shape Memory Alloys (SMAs) have the possibility to act as actuators and sensors which are integrated into composite structures, enabling new opportunities for designers and engineers. In this work, a finite element model and manufacturing process are used to model and manufacture demonstration SMAHC structures using novel methods. The demonstration case used in finite element modelling reveals 6.4 [%] change in curvature is possible using SMA actuation. The manufacturing fixture is used to demonstrate an electrical isolation scheme which prevents intimate contact of the SMAs with the carbon fibres. This modelling and manufacturing work enables the use commercially available FE tools and composites manufacturing techniques to be leveraged in the implementation of SMAHCs in industry.

Corresponding author: Pascal.hubert@mcgill.ca

SAMPE neXus Proceedings. Virtual Event, June 29 – July 1, 2021.
Society for the Advancement of Material and Process Engineering – North America.

1. INTRODUCTION

Despite performance advantages of composite materials, cost suppresses their widespread application. As such, research focus is often placed on driving down manufacturing times and cost [1], [2]. An alternative approach is to add value through adding functionality to their basic ability to bear load. Morphing hybrid composites add actuation into applications where it would not typically fit, opening design possibilities and adding value. Take for example, Boeing's Variable Geometry Chevron [3] which integrates a shape memory alloy actuator into a jet engine chevron. The tight volume of this application prevents a traditional actuator (i.e. electric or hydraulic actuator) from being used. Other applications where hybrid composites can enable morphing where traditional actuators cannot fit include quadcopter rotor blades or racing sailboat hydrofoils [4]. The morphing technology explored herein is a combination of nickel titanium-based shape memory alloys (SMAs), carbon fibre, and epoxy matrix hybrid composites. SMAs can be heated using the Joule effect to generate actuation forces and can also be used as sensors in a feedback loop [5]. Shape memory alloys hybrid composites (SMAHCs) have the potential to transform aeroelastic tailoring from passive to active in nature. Aspirationally, this technology could one day be used to realize NASA's vision of an integrated morphing wing (Figure 1) [6]. In this work, a demonstration of a SMAHC finite element model is shown, and a new manufacturing fixture is presented.

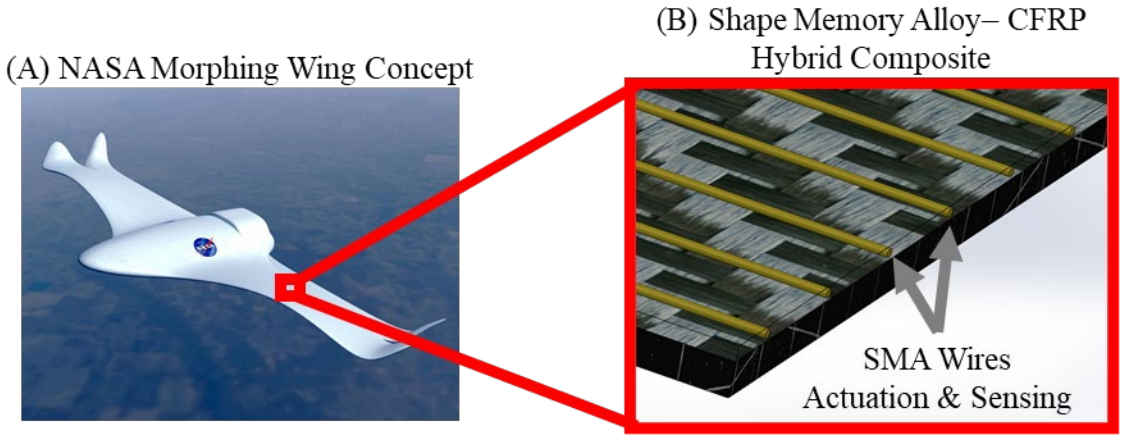

Figure 1 SMA Hybrid Composite (B) Used in NASA Morphing Wing Concept (A)NASA Morphing Wing available with open license [7] at [8]

2. SHAPE MEMORY ALLOYS

The SMAs used in this work are a nickel-titanium-copper alloy (NiTiCu). For actuation applications, the useful effect is superelasticity, with finite element and experimental responses for two temperatures shown in Figure 2. To use an SMA to actuate a structure, it must be pre-strained into the low stiffness plateau region (between 0.03 and 0.06 [mm/mm]) and affixed to the structure. By heating the SMA, the plateau stress increases (see Figure 2) and applies an actuation stress of 10.8 [MPA/°C] [11]. Additional characterization work, including that of low-cycle fatigue effects, is done by S. Iyer and P. Hubert in [11]. S. Iyer and P. Hubert find that this SMA wire needs to be cyclically loaded 43 times to stabilize its superelastic response prior to integration into structures.

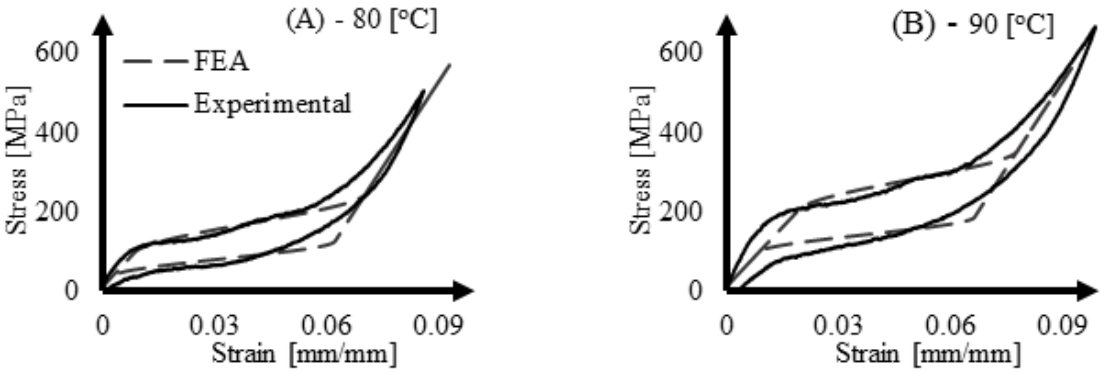

Figure 2 Finite Element & Experimental Superelastic Responses for 80 (A) and 90 (B) [°C] [11]

3. FINITE ELEMENT MODEL

The finite element model used is developed by S. Iyer [9]. To represent the non-linear thermally dependent orthotropic elastic behaviour, a four-node reduced-integration shell element (S4R) is used to represent the linear elastic components (FRP and adhesive layer). The SMA wires, whose behaviours are discussed in Section 2, are modelled using beam elements with the Auricchio & Taylor model [10] using properties for stabilized NiTiCu measured by S. Iyer and P. Hubert in [11]. The adhesive layer is FM-300 [12] and the composite used is NCT-301[13] [14].

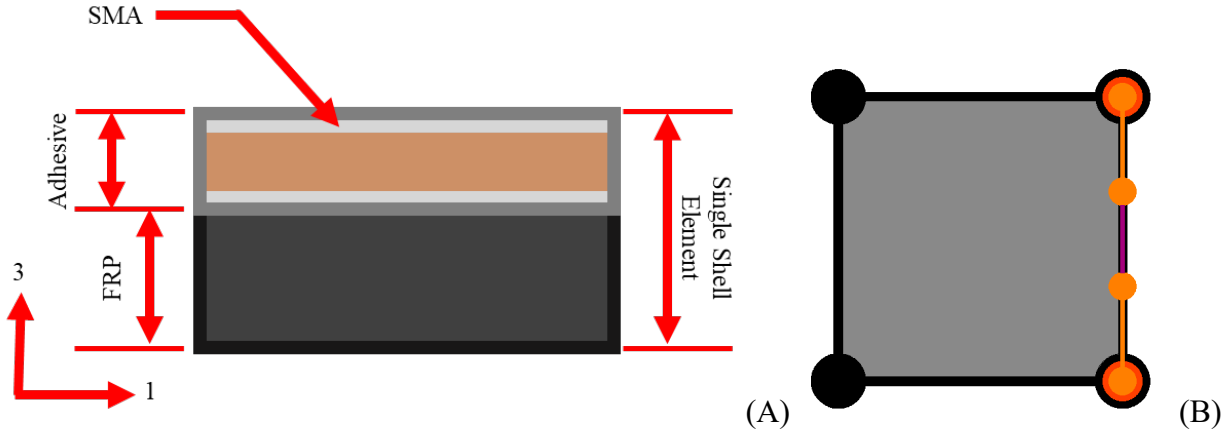

Figure 3 (A) Cross sectional representation of SMAHC and (B) unit cell of SMAHC laminate and with the S4R shell in grey with black nodes, B31H beam in orange, prestrained B31H beam in purple, and kinematic coupling constraints in red

4. MODEL SET UP & ANALYSIS METHODS

The demonstration model is setup as a 150 x 150 [mm] square with SMA wires running along the 1 direction of the panel. The layup used is $\{SMA + FM300 / 45 / -45 / 45 / 45\}_T$. In the SMA layer, 41 wires are included with spacing of 2.5 [mm]. The SMA wires are prestrained to 40 [με]. The boundary conditions applied to the panel are intended to prevent only rigid body motion of the panel, shown in Figure 4 and described as follows:

- Corner nodes one through four (CN1, CN2, CN3, & CN4) fixed in Z axis translation
- Corner nodes one and two (CN1 & CN2) fixed in Y axis translation
- Corner nodes one and three (CN1 & CN3) fixed in X axis translation

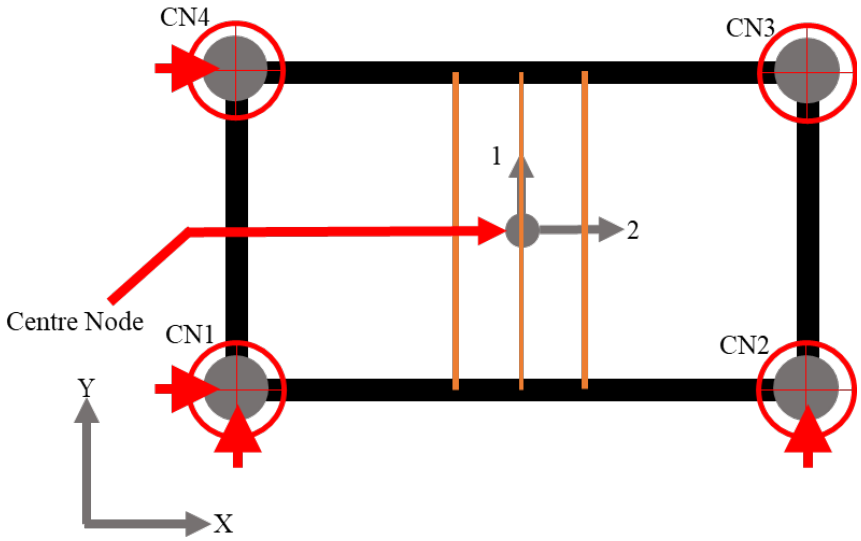

Figure 4 Parametric Study FE Model Boundary Condition and Load Setup

The loads applied to the panels are intended to simulate both the after curing effects and the behaviour under two separate load cases, SMA heating (actuation) and external out of plane loads. The load steps are broken down below:

0) Prestrain is applied to the SMAs
1) The laminate is cooled from gel temperature to a room temperature of 21 [°C] and the SMAs to the reference temperature (see T_0 in [11].)
2) The SMA wires are then heated to $T_{SMA} = 95\ [^oC]$ to simulate actuation
3) Lastly, a load is applied to the centre node (see Figure 4) to simulate out of plane behaviour and measure the out of plane response

To measure the laminate response, the as-cured curvature, change in curvature due to actuation, and out-of-plane displacement of the centre node are used. Equation 1 defines the laminate curvature in term of the geometric parameters shown in Figure 5. The as-cured curvature (κ_i^{AC}, see Equation [3]) captures the shape of the laminate due to residual stress from thermal shrinkage as well as the prestrain of SMAs in steps 0→1. The change in curvature ($\Delta\kappa_i^{AW}$, see Equation [3]) expresses the actuation available from heating the SMAs in step 2. Out-of-plane is used to represent he high degree of non-linearity in response to out of plane loading in the third step.

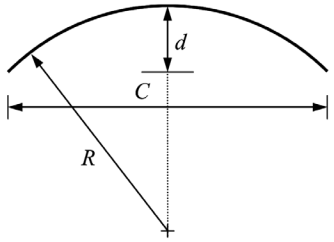

Figure 5 Curvature Measurement[1]

A_e	Surface area of shell element
C	Width of arc between end points
d	Depth of arc from peak to end point along radial direction
κ	Curvature
κ_{AC}	As cured curvature
κ_{AW}	Area weighted curvature
Subscript e	Denotes elemental measurement (as opposed to global)
T_{Heat}	Temperature to which SMA is heated for actuation
T_{SMA}	Temperature of SMA wires
T_0	Is SMA reference temperature from in [11]

$$\kappa = \frac{1}{R} = \frac{8d}{C^2 + 4d^2} \quad \text{Equation [1]}$$

$$\kappa^{AW} = \frac{\sum_{e=1}^{\infty} \kappa_e A_e}{\sum_{e=1}^{\infty} A_e} \quad \text{Equation [2]}$$

$$\kappa^{AC} = \kappa^{AW}|_{T_{SMA}=T_0} \quad \text{Equation [3]}$$

$$\Delta\kappa^{AW} = \frac{\kappa^{AW}|_{T_{SMA}=\mathrm{T_{Heat}}} - \kappa^{AC}}{\kappa^{AC}} * 100\ [\%] \quad \text{Equation [4]}$$

[1] As a visualization aid, the curvature of a soda can is approximately 30 [m^{-1}] or 0.030 [mm^{-1}]

5. FINITE ELEMENT RESULTS DISCUSSION

The 1st axis curvature response is shown in Figure 6. In the initial state, without any loads, the plate is flat. In the first step, when prestrain is applied, a gentle curvature is observed, which is expected as the SMA wires are on the surface of the layup. The curvature becomes more significant during the cooling from cure temperature to room temperature due to the orthotropic thermal expansion. Further curvature is created when the SMA is heated, due to the increase in applied stress of the SMA. During load application at the centre node, the laminate is observed to buckle (Figure 6 3.0) and take on a curved shape after buckling (Figure 6 3.1), similar to snap through behaviours of bistable laminates [15].

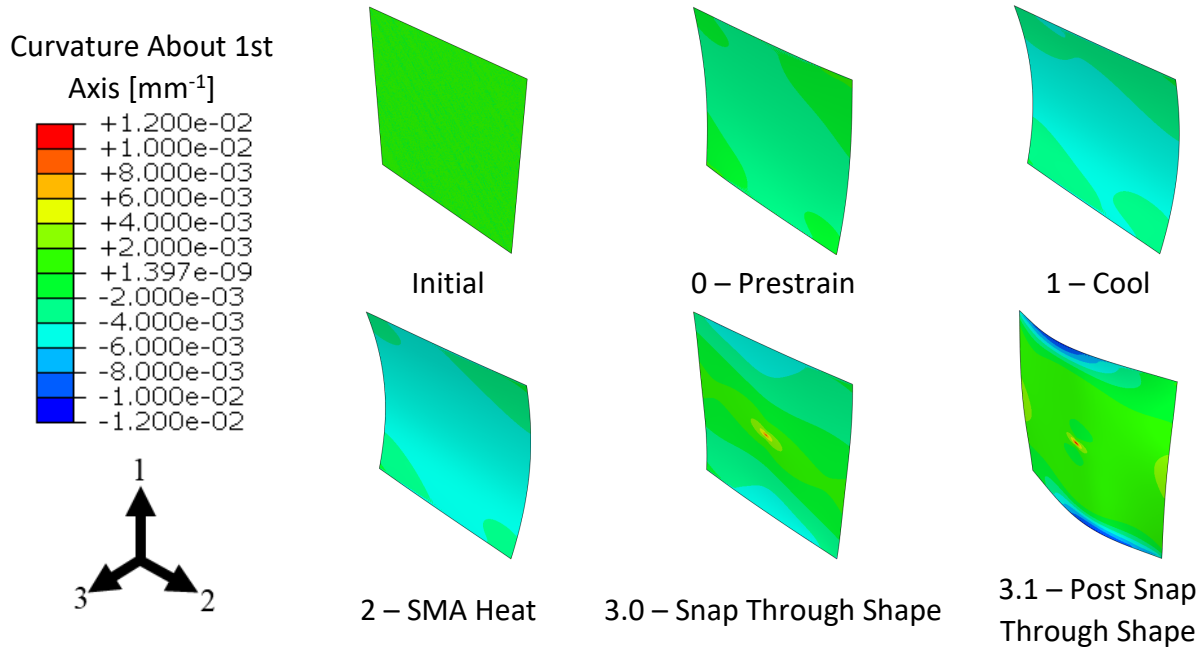

Figure 6 Demonstration Case Finite Element Curvature Results

A quantitative representation of this response is shown in Figure 7, with a focus on the actuation step. Prior to actuation, the initial curvature of this panel is 0.0041 [mm^{-1}] Upon heating the SMA, no curvature change is observed until 87 [ºC]. This initial lack of change is likely due to the hysteresis of the SMA wire and the structural stiffness of the panel. Once the threshold temperature is reached, the panel begins to bend with a linear stress-temperature response. The the SMA $\sigma(T)$ response is defined as linear, so the linear curvature response to temperature is consistent with expectations. This linear response is useful as it simplifies the future design of control systems. For this case, it is observed that a 6.4 [%] change in curvature is possible. Given the initial curvature, this a potentially significant change in terms of changing the shape of an aerostucture.

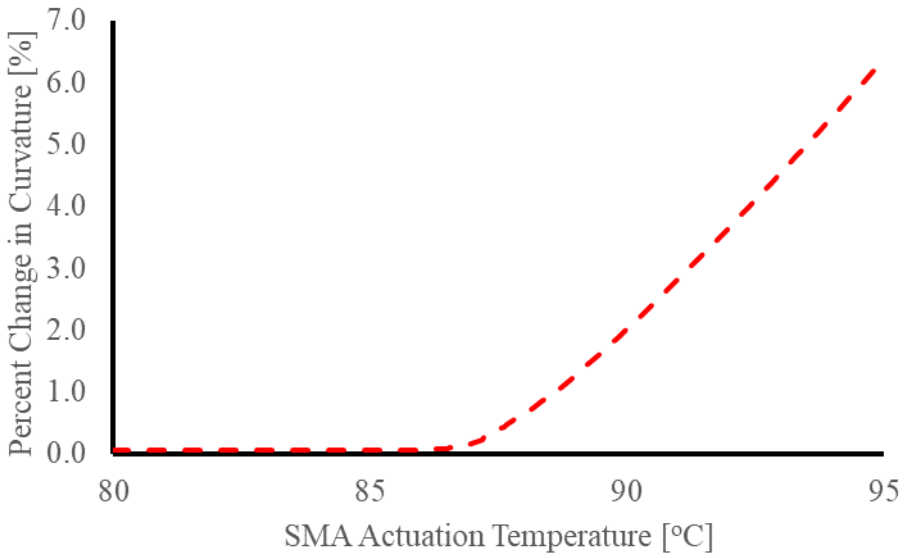

Figure 7 Percent Change in Curvature About 1st Axis vs. SMA Actuation Temperature for Demonstration Case

The demonstration case shows three key states, curvature introduced during the prestrain steps, the curvature and displacement due to the SMA heating, and the snap through response due to the unsymmetry of the laminate. This case demonstrates the usefulness of this model to simulating both manufacturing, actuation, and external loading of SMAHCs.

6. MANUFACTURING

The manufacturing of SMA hybrid composites is largely academic currently, which limits the usefulness and applicability of these techniques in industrial settings. A goal of this work is to review current techniques to inform the design of a new apparatus which solves issues. This is a preliminary work intended to lay the groundwork for in depth future SMAHC manufacturing.
Generally speaking, there are three categories for processing of SMAHCs, unstrained (at any temperature) and strained while processed below the SMA martensite finish temperature (M_f) or above the SMA Austenite finish temperature (A_f) (see [9] for a detailed discussion). Each combination of these conditions yields unique mechanical responses with varying challenges. The first category, SMAHCs with unstrained SMAs (herein referred to as UHCs for ***u**nstrained **h**ybrid **c**omposites*) do not provide the ability to create actuated structures as there is no prestrain. UHCs are typically used SMAs to improve impact damage tolerance [16], [17]. These structures are can be manufactured relatively simply, as they just involve attaching SMAs to composites. Secondly, are composites where processing is done below the SMA's M_f while prestrained (herein referred to as SLHCs for *pre**s**trained **l**ow-temperature **h**ybrid **c**omposites*), a technique comprehensively studied by [18]. Others have used this technique include [19]–[23]. This process allows SMAs to be prestrained then co-molded with or bonded to the composite while still in the shape memory regime. This removes the need for fixtures which maintain prestrain during cure. However, fixtures are still required for initially prestraining SMAs and positioning them during cure. Designing SLHCs involves consideration to ensure matrix performance will not degrade at temperatures at which the wire will be activated, limiting possibilities for SLHCs. The last option is processing the composite above the SMA's A_f while strained (herein referred to as SHHCs for *pre**s**trained*

***h**igh-temperature **h**ybrid **c**omposites*). SHHCs are the most complex to manufacture from a fixture perspective, as the mold must maintain wire position and prestrain at elevated temperatures. The trade-off is that since the SMAs are restrained, any matrix can be used (i.e. $T_{Gel} > A_f$). This allows the use of any SMA and composite, including those already used in aerospace applications. A fixture which restrains the wires during the curing process is required, and can add considerable complexity as in [24].

Hebda et. Al. [25] show void agglomeration around SMAs can be reduced by autoclave processing, so a fixture which enables the application of consolidation pressure (i.e. a vacuum bag or autoclave), so compatibility with a consolidation technique is imperative for SMAHCs as well.

6.1. Electrical Isolation of SMAs in SMAHCs

Given that both carbon fibres and SMAs are electrically conductive, there is an opportunity for galvanic corrosion to occur. Furthermore, SMAHC actuation is controlled using electrical current. Therefore, it's important that the SMAs are electrically insulated from the carbon fibres to ensure long term SMAHC performance. It is clear that any consolidation pressure applied to SMA composites will cause the SMA to come into close proximity, and likely contact, with the carbon fibres (see microscopy from [26] and [27]) which will cause electrical contact issues. Herein lies the purpose goal of the electrical isolation layer, to prevent contact of the SMA and carbon fibres to minimize current leakage.

There are several ways to provide electrical isolation. For this work, a fibre glass veil and an adhesive are used, as shown in Figure 8. The fibre glass veil and epoxy adhesive promote a uniform resin rich region near the SMA wires. This serves two purposes, first is to ensure the SMA is well molded into the composite. The second is to ensure the carbon fibres and SMAs remain separated. Thicker resin layers improve electrical isolation but worsen the mechanical properties.

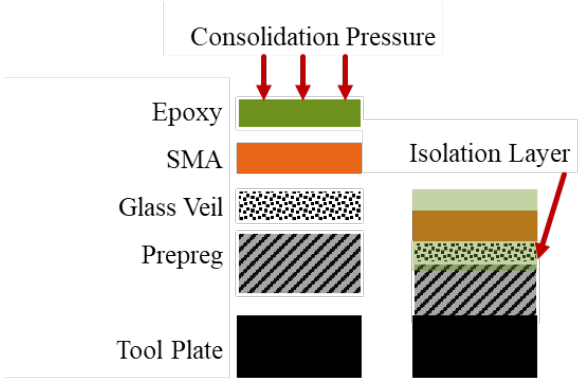

Figure 8 SMAHC Layup with Glass Veil for Electrical Isolation of SMA from CFRP

6.2. Electrical Isolation Testing

A rudimentary check is used to evaluate the electrical isolation of the panels, a schematic of which is shown in Figure 9. A DC voltage is applied to one end of a single wire using a Keithley 6221 power supply. A Keithley 2701 digital multimeter (DMM) is used to measure the current running through the circuit when the lead is applied to different SMA wires. This method identifies if two wires are in contact with the carbon fibre, so it must be repeated for all wire combinations. The positive terminal is fixed each wire, and the current is measured across each wire, with the number

of wires being (N), the number of measurements required is N^2. The DMM is capable of measuring signals on the order of [nA] [28], ensuring a useful measurement can be made.

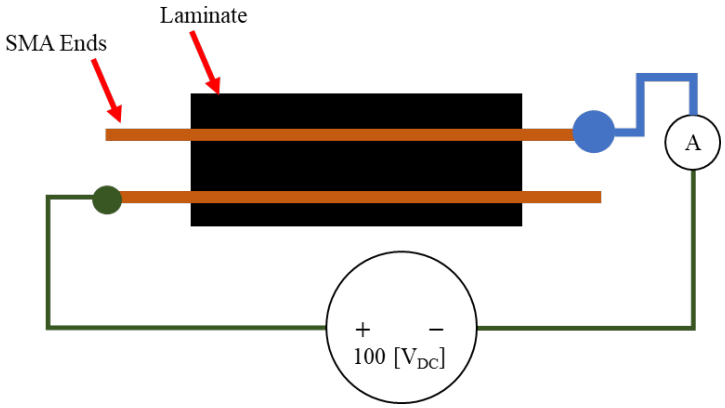

Figure 9 Schematic of Electrical Isolation Test

6.3. Existing Manufacturing Fixtures

SHHCs, though the most technically complex, is the most attractive as it allows readily available aerospace certified prepreg composites to be used. Firstly, this allows for precise ply orientation control offered by unidirectional prepregs – useful in elastically tailored structures. Secondly, using prepregs enables the use of existing processing techniques and infrastructure, such as autoclaves and ovens, allowing SHHCs to be more easily implemented. The work on manufacturing SHHCs is limited, even in academia. Turner et. Al. [29] use a tensile machine to apply prestrain and clamp the SMA ribbon to restrain it during cure. Another approach, used are fixtures, including those at École Polytechnique Fédérale de Lausanne (EPFL) [30] and at Loughborough University [31], which both prestrain SMA wires and restrain them during cure. The EPFL fixture (see Figure 100) uses wire-EDM cut combs to position the wires, enabling a high wire density of 500 [µm] between wires. Notable issues with both fixtures are the abilities to control SMA prestrain magnitude and equality, as well as the fact that they are both intended for use with cast resin systems. Controlling wire prestrain precisely is central to producing SMAHCs and is improved upon in this work.

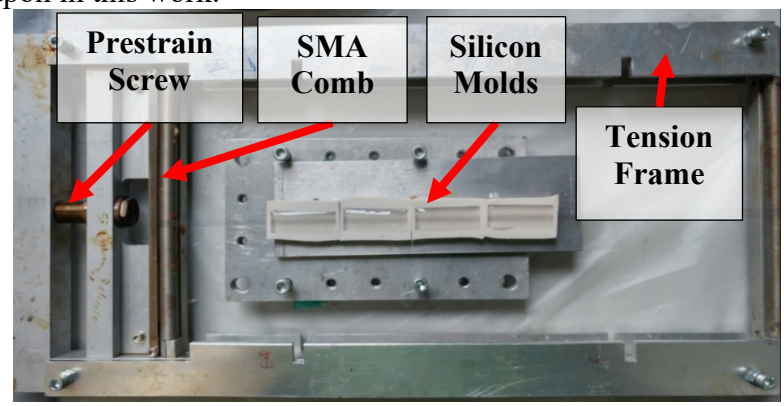

Figure 10 EPFL SMAHC Manufacturing Frame

6.4. New Manufacturing Fixture

The newly developed manufacturing fixture is shown in Figure 11. This fixture is designed to be used with vacuum bagging and out-of-autoclave prepregs and can be subject to temperatures as high as 260 [ºC] and allows the possibility for use with an autoclave (without the load cell). The key features of this fixture are:

1) The ACME lead screw for accurate and precise prestraining of the SMA wires
2) Combs for restraining SMA wires during cure with up to 80 wires 2 [mm/wire] spacing.
3) Combs are 2 [mm] deep, allowing layering of SMA wires as desired.
4) Combs have a 2 [mm] diameter round to allow for self-balancing tension between wires
5) An A2 steel tool plate with integrated vacuum ports to manufacture 250 x 250 [mm] panels
6) A custom die set with ball bearings to maintain smooth operation and rigidity
7) Custom brackets to precisely align the tool plate with the die set and SMA combs
8) A load cell for precisely measuring SMA preload up to 100 [kgf] total

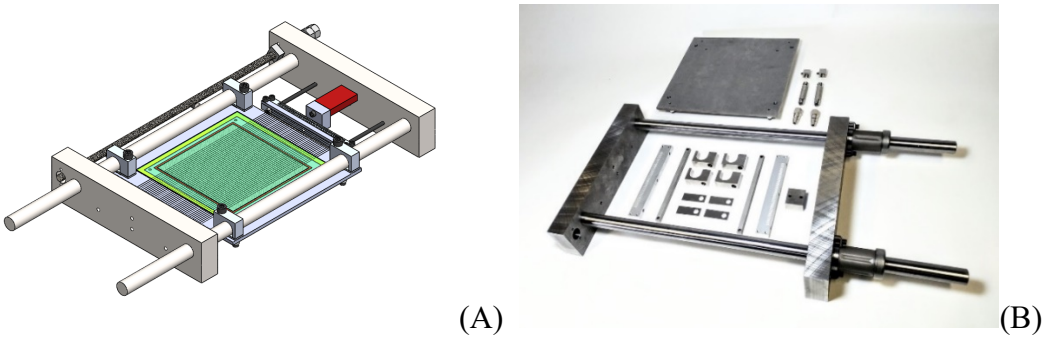

(A) (B)

Figure 11 SMAHC Manufacturing Fixture CAD (A) and Parts (B)

6.5. **Test Panel**

The purpose of manufacturing test panels for this work is to confirm the fixture functionality as well as confirming the electrical isolation of the wires. An extensive experimental series is not conducted and is considered future work. Panels are manufactured using Stabilized NiTiCu1 , NCT-301 matrix, and 34-700 fibre. Either Owens Corning M524-C64 [142] glass veil and FM300-2U [143] adhesive film or with Vivian Regina Fibasil Genmat 12 [mil] [34] glass veil and FM300U [145] adhesive film. Both Fibasil and Owens-Corning glass veils use C-Glass with areal weights of 30 [gsm], and similar binder contents, with the Fibasil having a 16 [µm] fibre diameter and the Owens Corning having one of 12.5 [µm]. A total of four panels were manufactured. No non-zero measurements were made for amperage in 3 of the 4 panels, indicating that the glass-veil and epoxy separation technique worked correctly. SMA-CFRP contact occurred between 4 of 20 wires in the first panel due to the glass veil shifting during consolidation.

An example test panel, shown in Figure 12. Note the void agglomeration around the SMA wire (consistent with observations by Hebda et. Al. [25]), and wicking of epoxy along the SMA wires. This first panel confirms the utility of the manufacturing fixture in maintaining SMA wire position as well as electrical isolation of the adhesive-glass veil approach.

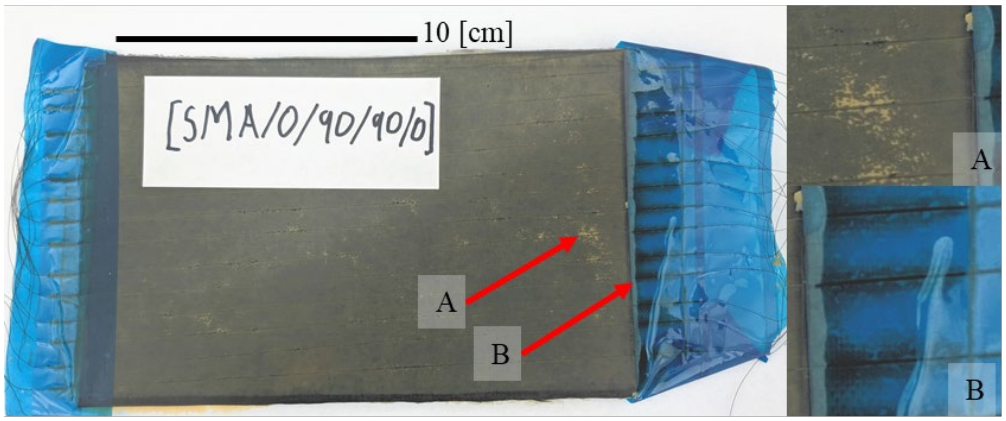

Figure 12 Test Panel 2 – Stabilized NiTiCu1 and FM300-2U with NCT-301 Matrix, 34-700 Fibre, and Owens Corning M524-C64 Glass Veil cured using the cycle from [36]. A wire spacing of 4 [mm/wire] is used Detail A showing void agglomeration around SMA and Detail B showing epoxy wicking along SMA.

7. CONCLUSIONS

In this work a finite element model is used to demonstrate the ability to simulate, using commercial finite element software, the response of SMAHC laminates to processing, actuation, and external loads. It's shown that useful actuation is possible, but designers must be careful in studying the out of plane response as it is highly non-linear. A new manufacturing fixture which enables the manufacturing of SHHC SMAHCs is built and tested. This fixture confirms the viability of the proposed electrical isolation scheme. The demonstrator panels are built as pre-cursors for a full experimental series to validate the finite element model.

8. ACKNOWLEDGEMENTS

The authors would like to thank their funding partners at the National Science and Engineering Research Council of Canada (NSERC), the Werner Graupe Chair, and the search Center for High Performance Polymer and Composite Systems (CREPEC). Additionally, Prof. Veronique Michaud at École polytechnique fédérale de Lausanne (EPFL) and Prof. Simon Joncas at École de technologie supérieure (ÉTS) for generously hosting the author and allowing them to conduct experimental work in their facilities.

9. REFERENCES

[1] "Chapter 6: Innovating Clean Energy Technologies in Advanced Manufacturing Technology Assessments, Composite Materials," United States Department of Energy, 2015.

[2] "FACT SHEET: President Obama Announces New Manufacturing Innovation Hub in Knoxville, Tennessee," *whitehouse.gov*, 09-Jan-2015. [Online]. Available: https://obamawhitehouse.archives.gov/the-press-office/2015/01/09/fact-sheet-president-obama-announces-new-manufacturing-innovation-hub-kn. [Accessed: 26-May-2019].

[3] F. Calkins, G. Butler, and J. Mabe, "Variable geometry chevrons for jet noise reduction," presented at the 12th AIAA/CEAS Aeroacoustics Conference (27th AIAA Aeroacoustics Conference), 2006, p. 2546.

[4] B. L. Giuntoli, "Design and validation of a non-linear passive-selective compliant hydrofoil using shape-memory alloys," masters, École de technologie supérieure, 2017.

[5] K. Ikuta, "Micro/miniature shape memory alloy actuator," in *, IEEE International Conference on Robotics and Automation Proceedings*, 1990, pp. 2156–2161 vol.3, doi: 10.1109/ROBOT.1990.126323.

[6] "NASA - NASA's Twist-wing Jet Explores A Radical Future." [Online]. Available: https://www.nasa.gov/missions/research/twist_wing.html. [Accessed: 06-Nov-2019].

[7] G. Daines, "Media Usage Guidelines," *NASA*, 11-Mar-2015. [Online]. Available: http://www.nasa.gov/multimedia/guidelines/index.html. [Accessed: 06-Nov-2019].

[8] "Morph ED01-0348-1: An artist's rendering of the 21st Century Aerospace Vehicle, sometimes nicknamed the Morphing Airplane, shows advanced concepts NASA envisions for an aircraft of the future." [Online]. Available: https://www.dfrc.nasa.gov/Gallery/Photo/Morph/HTML/ED01-0348-1.html. [Accessed: 06-Nov-2019].

[9] Sanesh Iyer, "Characterization, Modelling, and Manufacturing of Morphing Shape Memory Alloy Hybrid Composites," McGill University, 2019.

[10] Dassault Systemes, "Superelasticity," *SIMULIA User Assistance*, 2018. [Online]. Available: https://help.3ds.com/2018x/english/dsdoc/SIMA3DXMATRefMap/simamat-c-superelasticity.htm.

[11] Sanesh Iyer and Pascal Hubert, "Material Characterization of Shape Memory Alloys for Morphing Hybrid Composites," presented at the 11th Canadian International Conference on Composites, Kelowna, B.C., Canada, 2019.

[12] "Composite Materials for Aircraft Structures (2nd Edition) - Knovel." [Online]. Available: https://app.knovel.com/web/toc.v/cid:kpCMASE001/viewerType:toc//root_slug:composite-materials-for?kpromoter=marc&toc-within=cte%20fm300. [Accessed: 18-Mar-2019].

[13] R. Ganesan and A. Zabihollah, "Vibration analysis of tapered composite beams using a higher-order finite element. Part II: parametric study," *Compos. Struct.*, vol. 77, no. 3, pp. 319–330, Feb. 2007, doi: 10.1016/j.compstruct.2005.07.017.

[14] Inn B Kim, "Development and Analysis of Elastically Tailored Composite Stare Shaped Beam Sections," Georgia Institute of Technologiy, 2003.

[15] S. Anwar Tawfik, *Stability and morphing characteristics of bistable composite laminates*. 2008.

[16] R. L. Ellis, F. Lalande, H. Jia, and C. A. Rogers, "Ballistic Impact Resistance of SMA and Spectra Hybrid Graphite Composites," *J. Reinf. Plast. Compos.*, vol. 17, no. 2, pp. 147–164, Jan. 1998, doi: 10.1177/073168449801700205.

[17] K. S. C. Kuang and W. J. Cantwell, “The use of plastic optical fibres and shape memory alloys for damage assessment and damping control in composite materials,” *Meas. Sci. Technol.*, vol. 14, no. 8, pp. 1305–1313, Jul. 2003, doi: 10.1088/0957-0233/14/8/316.
[18] Kirkby, Eva, “Active Sensing and Repair Composites,” Docteur Es Sciences, Ecole Polytechnique Federale de Lausanne, Lausanne, Switzerland.
[19] M.-S. Kim, W.-S. Chu, J.-H. Lee, Y.-M. Kim, and S.-H. Ahn, “Manufacturing of inchworm robot using shape memory alloy (SMA) embedded composite structure,” *Int. J. Precis. Eng. Manuf.*, vol. 12, no. 3, pp. 565–568, Jun. 2011, doi: 10.1007/s12541-011-0071-2.
[20] S. R. White and J. B. Berman, “Thermomechanical response of SMA composite beams with embedded nitinol wires in an epoxy matrix,” *J. Intell. Mater. Syst. Struct.*, vol. 9, pp. 391–400, 1998.
[21] H. Rodrigue, W. Wang, B. Bhandari, M.-W. Han, and S.-H. Ahn, “Cross-shaped twisting structure using SMA-based smart soft composite,” *Int. J. Precis. Eng. Manuf.-Green Technol.*, vol. 1, no. 2, pp. 153–156, Apr. 2014, doi: 10.1007/s40684-014-0020-5.
[22] Zafar Adeel and Andrawes Bassem, “Fabrication and Cyclic Behavior of Highly Ductile Superelastic Shape Memory Composites,” *J. Mater. Civ. Eng.*, vol. 26, no. 4, pp. 622–632, Apr. 2014, doi: 10.1061/(ASCE)MT.1943-5533.0000797.
[23] H. Rodrigue, W. Wei, B. Bhandari, and S.-H. Ahn, “Fabrication of wrist-like SMA-based actuator by double smart soft composite casting,” *Smart Mater. Struct.*, vol. 24, no. 12, p. 125003, Oct. 2015, doi: 10.1088/0964-1726/24/12/125003.
[24] “(1) (PDF) Progress on Composites with Embedded Shape Memory Alloy Wires,” *ResearchGate*. [Online]. Available: https://www.researchgate.net/publication/37436627_Progress_on_Composites_with_Embedded_Shape_Memory_Alloy_Wires. [Accessed: 12-Jun-2019].
[25] D. A. Hebda, M. E. Whitlock, J. B. Ditman, and S. R. White, “Manufacturing of Adaptive Graphite/Epoxy Structures with Embedded Nitinol Wires,” *J. Intell. Mater. Syst. Struct.*, vol. 6, no. 2, pp. 220–228, Mar. 1995, doi: 10.1177/1045389X9500600209.
[26] X. Ya, K. Otsuka, N. Toyama, H. Yoshida, H. Nagai, and T. Kishi, “A novel technique for fabricating SMA/CFRP adaptive composites using ultrathin TiNi wires,” *Smart Mater. Struct.*, vol. 13, p. 196, 2004.
[27] B. K. Jang and T. Kishi, “Adhesive strength between TiNi fibers embedded in CFRP composites,” *Mater. Lett.*, vol. 59, no. 11, pp. 1338–1341, May 2005, doi: 10.1016/j.matlet.2005.01.006.
[28] K. I. Inc, “Model 2701 Ethernet-Based DMM/Data Acquisition System User’s Manual,” p. 506.
[29] T. L. Turner, C. L. Lach, and R. J. Cano, “Fabrication and characterization of SMA hybrid composites,” in *Smart Structures and Materials 2001: Active Materials: Behavior and Mechanics*, 2001, vol. 4333, pp. 343–354, doi: 10.1117/12.432774.
[30] V. Michaud, “Can shape memory alloy composites be smart?,” *Scr. Mater.*, vol. 50, pp. 249–253, 2004.
[31] G. Zhou and P. Lloyd, “Design, manufacture and evaluation of bending behaviour of composite beams embedded with SMA wires,” *Compos. Sci. Technol.*, vol. 69, no. 13, pp. 2034–2041, Oct. 2009, doi: 10.1016/j.compscitech.2009.01.017.
[32] “Product Information M524-C64 Surfacing Tissue for GRP Laminates.” Owens Corning\.
[33] “TECHNICAL DATA SHEET FM 300-2 ADHESIVE FILM.” Solvay.
[34] “FIBASIL.” Vivian Regina.

[35] “TECHNICAL DATA SHEET FM 300 ADHESIVE FILM.” Solvay.
[36] “Newport 301 Product Data Sheet.” Mitsubishi Rayon Carbon Fiber and Composites, Inc, 2012.